

# SCIENTIFIC REPORTS



OPEN

## Targeting Thioredoxin-1 by dimethyl fumarate induces ripoptosome-mediated cell death

Anne Schroeder<sup>1</sup>, Uwe Warnken<sup>2</sup>, Daniel Röth<sup>1</sup>, Karel D. Klika<sup>3</sup>, Diana Vobis<sup>1</sup>, Andrea Barnert<sup>1</sup>, Fatmire Bujupi<sup>1</sup>, Tina Oberacker<sup>1</sup>, Martina Schnölzer<sup>2</sup>, Jan P. Nicolay<sup>1,4</sup>, Peter H. Krammer<sup>1</sup> & Karsten Gülow<sup>1</sup>

Received: 26 October 2016

Accepted: 20 January 2017

Published: 24 February 2017

Constitutively active NF $\kappa$ B promotes survival of many cancers, especially T-cell lymphomas and leukemias by upregulating antiapoptotic proteins such as inhibitors of apoptosis (IAPs) and FLICE-like inhibitory proteins (cFLIPs). IAPs and cFLIPs negatively regulate the ripoptosome, which mediates cell death in an apoptotic or necroptotic manner. Here, we demonstrate for the first time, that DMF antagonizes NF $\kappa$ B by suppressing Thioredoxin-1 (Trx1), a major regulator of NF $\kappa$ B transcriptional activity. DMF-mediated inhibition of NF $\kappa$ B causes ripoptosome formation *via* downregulation of IAPs and cFLIPs. In addition, DMF promotes mitochondrial Smac release and subsequent degradation of IAPs, further enhancing cell death in tumor cells displaying constitutive NF $\kappa$ B activity. Significantly, CTCL patients treated with DMF display substantial ripoptosome formation and caspase-3 cleavage in T-cells. DMF induces cell death predominantly in malignant or activated T-cells. Further, we show that malignant T-cells can die by both apoptosis and necroptosis, in contrast to resting T-cells, which are restricted to apoptosis upon DMF administration. In summary, our data provide new mechanistic insight in the regulation of cell death by targeting NF $\kappa$ B *via* Trx1 in cancer. Thus, interference with Trx1 activity is a novel approach for treatment of NF $\kappa$ B-dependent tumors.

Nuclear factor- $\kappa$ B (NF $\kappa$ B) is a central transcription factor orchestrating innate and adaptive immune responses. In acute inflammation, NF $\kappa$ B activity is tightly regulated. However, aberrantly activated NF $\kappa$ B is associated with chronic inflammatory diseases and a variety of human cancers including both solid and hematopoietic malignancies. Cancers such as T-cell acute lymphoblastic leukemia (T-ALL), cutaneous T-cell lymphoma (CTCL), and its leukemic variant, Sézary Syndrome, revealed constitutive NF $\kappa$ B activity<sup>1–4</sup>.

The NF $\kappa$ B family consists of five Rel related proteins: RelA (p65), RelB, cRel, p50 and p52, which can form both homo- and heterodimers. The typical NF $\kappa$ B complex is a p65/p50 heterodimer critical for NF $\kappa$ B mediated anti-apoptotic effects<sup>5</sup>. In its inactive form, NF $\kappa$ B is sequestered in the cytoplasm by I $\kappa$ B $\alpha$ . Phosphorylation and proteasomal degradation of I $\kappa$ B $\alpha$  releases NF $\kappa$ B. Subsequent nuclear translocation and full activation of NF $\kappa$ B is redox-dependent and mediated by phosphorylation<sup>6</sup>. The redox regulator Thioredoxin-1 (Trx1) promotes DNA binding activity of NF $\kappa$ B by reduction of a cysteine residue within its DNA binding domain<sup>7,8</sup>. During oncogenesis, NF $\kappa$ B promotes cell survival and proliferation by inducing expression of molecules associated with suppression of programmed cell death (PCD), such as cFLIPs<sup>9</sup>, IAP proteins<sup>6,10</sup>, and members of the Bcl-2 family<sup>11</sup>. PCD is a mechanism of tumor suppression and manifests itself in, *e.g.* apoptosis and necroptosis. Necroptosis is a form of regulated necrosis, which has been implicated to trigger strong immune responses by release of damage-associated molecular patterns (DAMPs)<sup>12</sup>. Moreover, necroptosis is critical for T-cell homeostasis as backup to eliminate an excess of activated T-cells after clonal expansion preventing autoimmunity<sup>13</sup>.

The ripoptosome is a signaling platform triggering cell death in an apoptotic or necroptotic manner<sup>14–16</sup>. The core components of the ripoptosome include caspase-8, FADD (Fas-associated death domain) and RIPK1 (Receptor-interacting kinase 1). Formation and activation of the ripoptosome are negatively regulated by IAPs (cIAP1, cIAP2 and XIAP) and cFLIPs (cFLIP<sub>L</sub> and cFLIP<sub>S</sub>), respectively. IAPs are regulated by Smac (Second

<sup>1</sup>Division of Immunogenetics, Tumor Immunology Program, German Cancer Research Center (DKFZ), Heidelberg, Germany. <sup>2</sup>Functional Proteome Analysis, German Cancer Research Center (DKFZ), Heidelberg, Germany. <sup>3</sup>Molecular Structure Analysis, German Cancer Research Center (DKFZ), Heidelberg, Germany. <sup>4</sup>Department of Dermatology, Venereology and Allergy, University Medical Center Mannheim, Mannheim, Germany. Correspondence and requests for materials should be addressed to K.G. (email: k.guelow@dkfz.de)

mitochondria-derived activator of caspases) released by mitochondria in response to pro-apoptotic stimuli. In the cytosol, Smac interacts and antagonizes IAPs. MOMP (mitochondrial outer membrane permeabilization)-associated Smac release is regulated by Bcl-2 family members<sup>17</sup>. The caspase-8 regulators cFLIPs modulate the ripoptosome response. While cFLIP<sub>L</sub> seems to suppress ripoptosome activity, overexpression of cFLIP<sub>S</sub> diminishes caspase-8 activity, thus, promoting necroptosis<sup>15</sup>. Notably, ripoptosome formation predominantly occurs in malignant cells<sup>16</sup>.

Evasion from PCD is a hallmark of cancer and facilitates immune escape, chemoresistance and poor prognosis. Regulators of PCD, such as IAPs, are frequently overexpressed in many cancer cells. Therefore, it is of great interest to design novel therapeutics targeting cell death resistant cancer cells. So far, several small molecule inhibitors have been developed to facilitate depletion of IAPs. Smac mimetics bind to IAPs leading to rapid auto-ubiquitylation and degradation<sup>18</sup>. Depletion of IAPs may also occur by chemotherapeutic drugs, which induce genotoxic stress such as etoposide<sup>19</sup>. Since IAPs, cFLIPs and Bcl-2 family members are target genes of NF $\kappa$ B, NF $\kappa$ B is an attractive target for cancer therapy. Clinically DMF is a promising therapeutic agent for CTCL since DMF has limited side effects compared to other NF $\kappa$ B inhibitors, which display relatively high toxicity<sup>2,20</sup>. However, the exact molecular mechanism of DMF-induced NF $\kappa$ B inhibition and subsequent cell death remains to be elucidated.

Here, we show that DMF (Tecfidera<sup>®</sup>), a FDA-approved drug for treatment of multiple sclerosis, blocks Trx1 activity by modification of a specific thiol group. Reduced Trx1 activity leads to inhibition of NF $\kappa$ B. Remarkably, DMF-mediated inhibition of the Trx1/NF $\kappa$ B axis results in ripoptosome formation and subsequent PCD by downregulation of cIAP2 and cFLIPs *in vitro* and *in vivo*. Full ripoptosome activation requires mitochondria and release of Smac. Cytosolic Smac promotes degradation of cIAP1 and XIAP, further enhancing ripoptosome formation and activation in an amplification loop. Moreover, DMF treated Sézary patients reveal ripoptosome assembly which coincides with caspase-3 cleavage. DMF administration induced cell death more efficiently in malignant CD4<sup>+</sup> T-cells isolated from Sézary patients compared to resting T-cells. Other than apoptosis which is induced in T-cells from Sézary patients and healthy donors, necroptosis predominantly occurs in malignant T-cells.

Hence, targeting the Trx1/NF $\kappa$ B signal transduction by DMF may represent a promising treatment for lymphoproliferative diseases. Our data further provide a rationale for the development of novel compounds treating NF $\kappa$ B dependent tumors.

## Results

**DMF suppresses activity of Trx1 by monomethyl succinylation.** DMF is a potent inhibitor of NF $\kappa$ B<sup>21</sup>, though the molecular mechanism by which DMF suppresses transcriptional activity of NF $\kappa$ B is unclear. DMF has been shown to modify reactive thiol groups in *e.g.* glutathione (Supplementary Data and Supplementary Fig. S1A)<sup>22</sup>. Together with glutathione, thioredoxin proteins (Trx1 and Trx2) control cellular reactive oxygen species (ROS). In addition, Trx1 controls the redox state of cysteine residues in proteins such as NF $\kappa$ B<sup>23</sup>. Therefore, we set out to determine whether inhibition of NF $\kappa$ B is mediated by DMF-dependent suppression of Trx1.

Mass spectrometry (MS) was used to identify chemical modifications of Trx1 in response to DMF. Interestingly, the redox sensitive cysteines (C32 and C35) have not been targeted. However, C73, which possesses a regulatory function controlling general activity of Trx1<sup>24–27</sup>, was identified as monomethyl succinylated (Fig. 1A, Supplementary Fig. S1B–D). Notably, we detected no modification of Trx2. Equal concentrations of MMF (25  $\mu$ M), a hydrolyzation product of DMF, did not result in detectable modifications of Trx1 (data not shown).

To investigate the impact of monomethyl succinylation activity of Trx1 was determined. Modification of Trx1 led to an inhibition of its activity. PMX464, a known Trx inhibitor<sup>28</sup>, was used as positive control (Fig. 1B). Furthermore, DMF-dependent suppression of Trx1 resulted in elevated levels of ROS. Treatment with trolox, a water-soluble vitamin E derivative and thiol-independent antioxidant, blocked DMF-dependent ROS accumulation (Fig. 1C). Thus, monomethyl succinylation of C73 by DMF inhibits Trx1 activity.

**NF $\kappa$ B inhibition by DMF induces loss of cIAP2 and cFLIP.** As a regulator of NF $\kappa$ B transcriptional activity Trx1 is an attractive target for cancer therapy. Trx1 promotes transcriptional activity of NF $\kappa$ B by reducing a cysteine in its DNA binding domain<sup>23</sup>. To evaluate the redox state of NF $\kappa$ B upon DMF treatment, proteins containing free thiols were precipitated. Inhibition of Trx1 in response to DMF led to a time-dependent accumulation of inactive/oxidized NF $\kappa$ B. Cysteines in NF $\kappa$ B were oxidized 2 h after DMF treatment (Fig. 2A). Similarly, PMX464 suppressed reduction of cysteines in NF $\kappa$ B (Supplementary Fig. S2A).

Oxidized cysteines in NF $\kappa$ B should result in diminished DNA binding. Therefore, we tested DNA binding of NF $\kappa$ B on target genes such as *Birc2*, *Birc3*, *Xiap*, *Cflar*, *Bcl-2* and *Bcl2l1*. DNA oligonucleotides with NF $\kappa$ B binding sites were pulled-down and probed for the presence of NF $\kappa$ B. DNA binding of NF $\kappa$ B to oligonucleotides of *Birc2*, *XIAP* and *Bcl-2* was not regulated in response to DMF. However, DMF treatment suppressed NF $\kappa$ B binding to *Birc3*, *Cflar* and *Bcl2l1* (Fig. 2B; Supplementary Fig. S2B). Consistently, DMF inhibited mRNA and protein expression of cIAP2 and cFLIPs (Fig. 2C,D). However, Bcl<sub>L</sub> expression was only moderately impaired on mRNA and protein level (Fig. 2C,D). Bcl-2 was not regulated in response to DMF (Fig. 2D; Supplementary Fig. S2C). Collectively, our data demonstrate that inhibitors of Trx1 such as DMF and PMX464 suppress reduction of cysteines in NF $\kappa$ B. DMF-dependent oxidation of cysteines in NF $\kappa$ B results in diminished expression of cIAP2 and cFLIPs (Supplementary Fig. S2D).

**Inhibition of NF $\kappa$ B activity results in ripoptosome formation.** NF $\kappa$ B inhibition by DMF caused cell death in HH, SeAx and CEM cells in a dose- and time-dependent manner (Supplementary Fig. S3A). Since Trx1 inhibition by DMF triggered ROS accumulation, we tested whether ROS is the source for cell death.

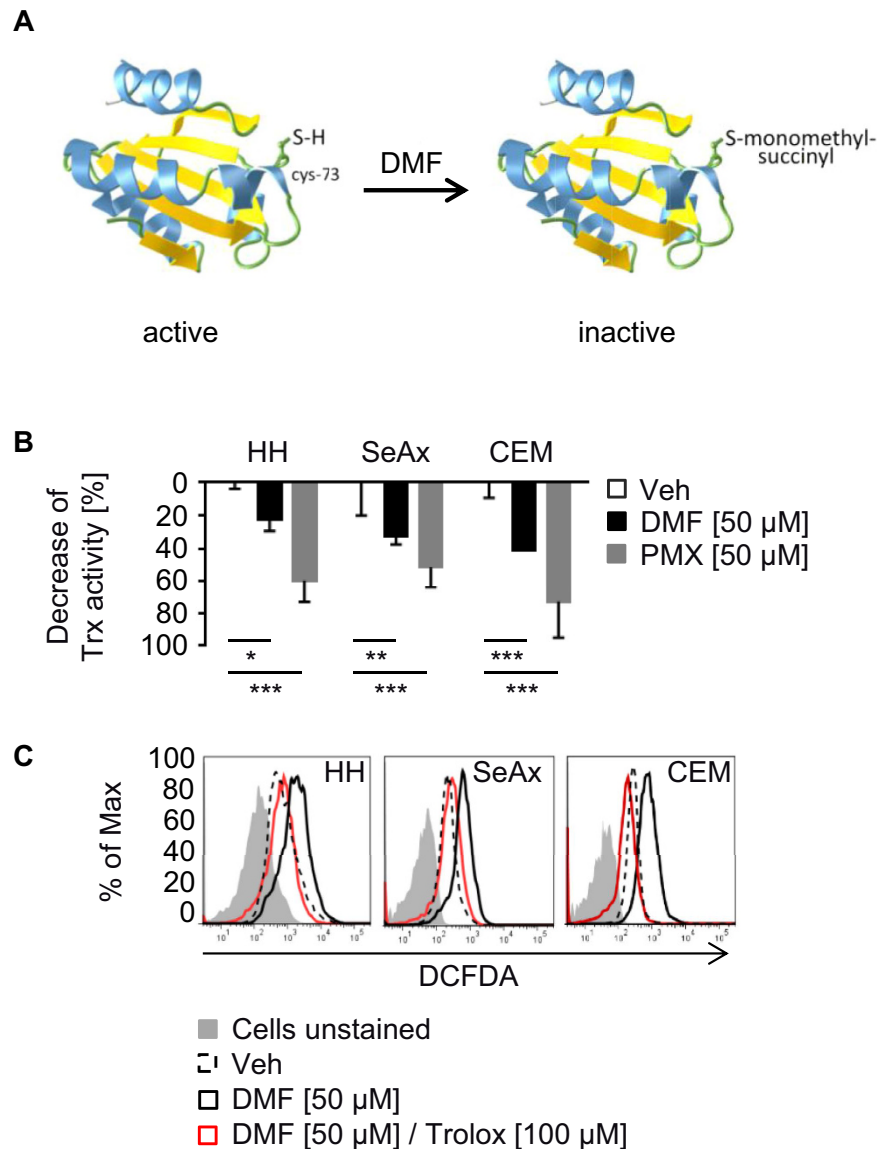


**Figure 1. DMF inhibits Trx1 activity.** (A) Trx1 is monomethyl succinylated at cysteine 73 (C73). To generate the 3D structure of Trx1 Aquaria database software (<http://aquaria.ws/>) was used<sup>49,50</sup>. (B) Trx activity of cells was measured 2 h after treatment with DMSO (Veh), DMF, or PMX464 (PMX) (n = 3). (C) HH, SeAx and CEM cells were left unstimulated or stimulated with DMSO (Veh), DMF or DMF and Trolox for 2 h. Untreated cells were left unstimulated. Treated cells were stained with H<sub>2</sub>DCFDA for 30 min and analyzed by flow cytometry. (B) Error bars represent standard deviation. Statistics were calculated using Student's t-test (\*p < 0.05; \*\*p < 0.005; \*\*\*p < 0.001).

However, cell death mediated by DMF was independent of ROS. Trolox diminished ROS accumulation upon DMF treatment (Fig. 1C), but failed to rescue DMF-induced cell death (Supplementary Fig. S3B). Thus, ROS and Iron-dependent cell death can be excluded<sup>29</sup>. Instead, cell death mediated by DMF was facilitated by caspase-8 and -3 activation (Fig. 3A; Supplementary Figure S3C). Importantly, activation of caspase-8 and -3 was independent of extrinsic death ligands. DMF failed to stimulate mRNA expression of CD95L, TNF $\alpha$  and TRAIL in malignant T-cells (Supplementary Fig. S4A). In addition, treatment with inhibitors for CD95L (APG101), TNF $\alpha$  (Enbrel) and TRAIL (TRAIL-Fc), either alone or in combination, had no effect on cell death induced by DMF (Supplementary Fig. S4B,C).

Since no extrinsic ligands were involved in caspase activation upon NF $\kappa$ B inhibition, we set out to determine whether an intrinsic cell death platform called the ripoptosome facilitates PCD. Ripoptosome formation is blocked by IAPs. Downregulation of IAPs upon DMF administration (Fig. 2D) coincided with elevated caspase-8 activity (Fig. 3A). It was reported that RIPK1 is negatively regulated by caspase-8 and FADD once incorporated in the ripoptosome complex. Active caspase-8 cleaves RIPK1 after D324, thus, promoting apoptosis but inhibiting necroptosis<sup>30</sup>. Consistent with DMF-induced kinetics of caspase-8 activation (Fig. 3A) RIPK1 was cleaved upon DMF administration (Fig. 3B; Supplementary Fig. S4D). Abrogation of caspase activity by zVad

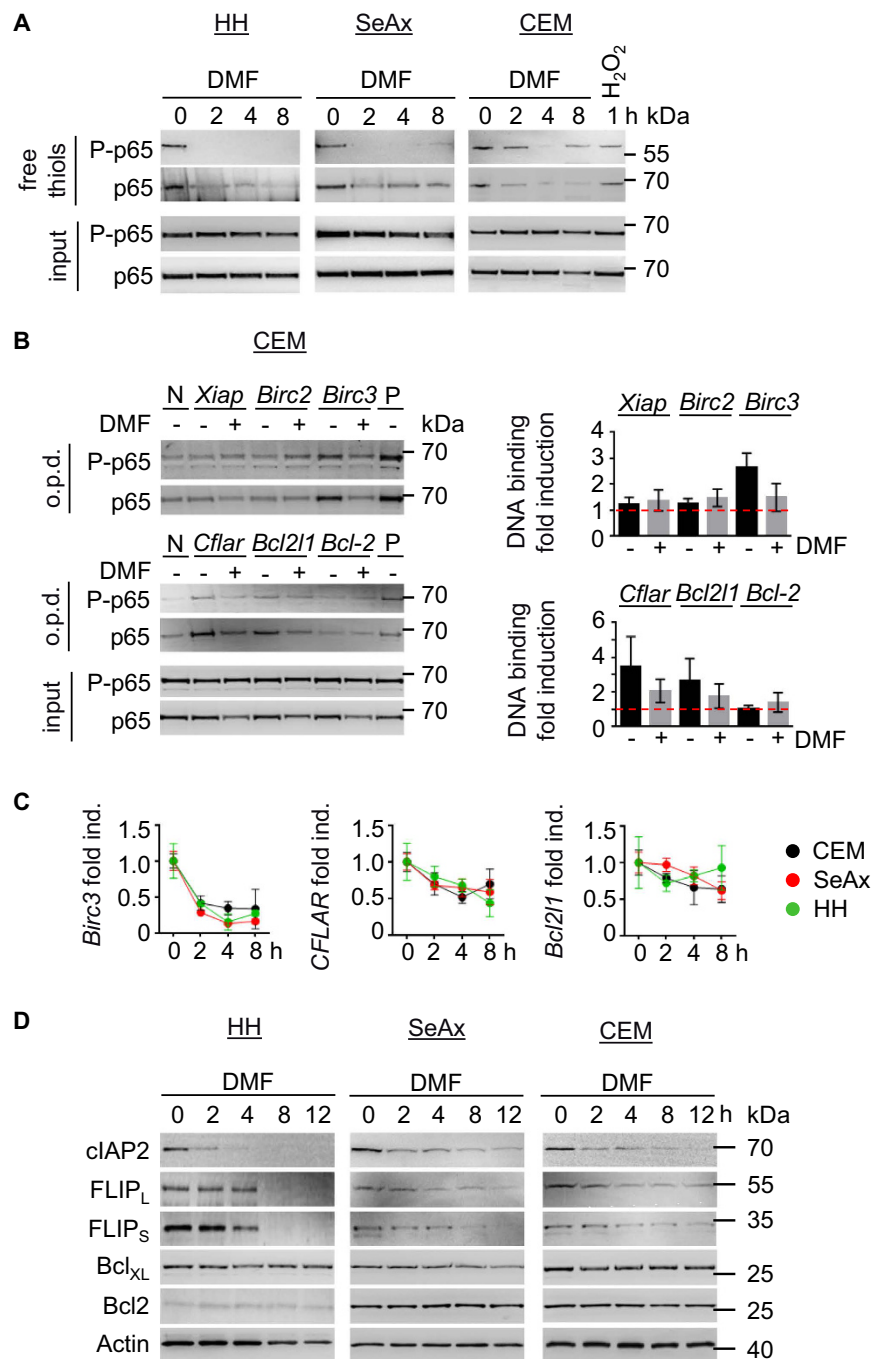


**Figure 2. DMF-dependent modification of Trx leads to inhibition of NF $\kappa$ B activity.** (A) Cells were treated with DMF (50  $\mu$ M) in a time-dependent manner as indicated. CEM cells were incubated with H<sub>2</sub>O<sub>2</sub> (100  $\mu$ M) for 2 h as positive control. Reduced proteins were pulled-down using biotinylated iodoacetamide (BIAM) and probed for phospho- and total NF $\kappa$ B. (B) CEM cells were left untreated or treated with DMF (50  $\mu$ M) for 4 h. NF $\kappa$ B DNA binding was assessed by oligo pull-down (o.p.d.) for indicated biotinylated oligonucleotides containing NF $\kappa$ B binding sites. Positive and negative controls are denoted by P or N respectively (left). Band intensities were quantified from 3 independent experiments and normalized to negative control (right). (C) Quantitative real-time PCR of indicated genes was performed in triplicates using RNA derived from cells treated with DMF (50  $\mu$ M) for 2, 4, and 8 h. (D) HH, SeAx and CEM cells were incubated with DMF (50  $\mu$ M) for the indicated time points. Cell lysates were analyzed by Western blot. (B,C) Error bars represent standard deviation.

application rescued RIPK1 cleavage in DMF treated cells suggesting complex formation of caspase-8 with RIPK1. As expected, loss of cIAP2 expression was not influenced upon zVad administration (Fig. 3B).

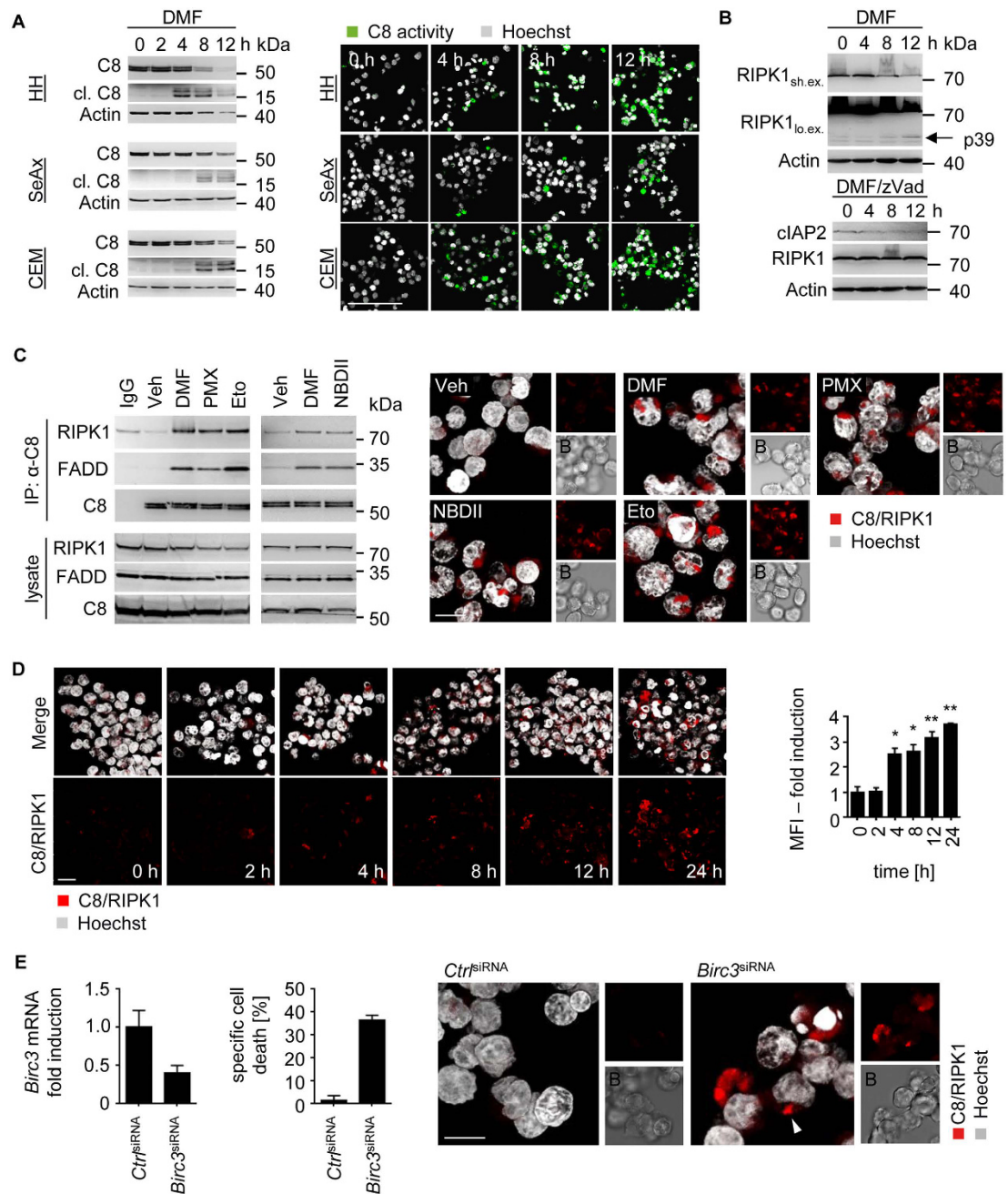


**Figure 3. Ripoptosome formation induced by DMF results in caspase-8-dependent cell death.** (A) CEM cells were treated with DMF (50  $\mu$ M) for the indicated time points. Caspase-8 (C8) cleavage was determined by Western blot (left), immunofluorescence (IF) shows cleaved caspase-8; for IF, Hoechst (grey), caspase-8 cleavage (green); scale bar, 100  $\mu$ m (right). (B) Western blot analysis of DMF (50  $\mu$ M) or DMF/zVad treated CEM cells. Cells were treated for the indicated time points (lo. ex. represents prolonged exposure of the blots; sh. ex. represents short exposure). (C) CEM cells were pre-incubated with zVad and Necrostatin-1 (Nec-1) for 30 min and then treated with DMSO (Veh), DMF (50  $\mu$ M), PMX464 (PMX, 1  $\mu$ M), etoposide (Eto, 50  $\mu$ M) or NBDII (50  $\mu$ M) for 16 h. Immunoprecipitation (IP) was performed with antibodies against caspase-8 ( $\alpha$ -C8). As negative control, DMF treated cells were incubated with goat IgG (left). Complex formation of caspase-8 (C8) and RIPK1 was analyzed by Proximity ligation assay (PLA). Depicted are z-stacks; Hoechst (grey), C8/RIPK1 (red), and Brightfield (B); scale bar, 10  $\mu$ m (right). (D) SeAx cells were treated with DMF (50  $\mu$ M) for the indicated time points. Interaction of RIPK1 and caspase-8 was determined by PLA (red), Hoechst (grey). Shown are representative confocal microscopy images and mean fluorescence intensities (MFI) (n = 3). (E) Knock-down of *Birc3* (cIAP2) results in ripoptosome-dependent cell death. siRNA-transfected CEM cells were analyzed by qPCR (left), specific cell death (middle), and PLA (right) (n = 3). Complexes of caspase-8 (C8) and RIPK1 are depicted in red and indicated with a white arrow, Hoechst (grey), Brightfield (B); scale bar, 10  $\mu$ m. (D, E) Error bars represent standard deviation. Statistics were calculated using Student's t-test (\*p < 0.05; \*\*p < 0.005; \*\*\*p < 0.001).

To elucidate ripoptosome assembly in response to DMF, we tested interaction of caspase-8 with RIPK1 and FADD using the proximity ligation assay. Fluorescent signals from interaction of caspase-8 with RIPK1 or FADD were detected in response to DMF (Supplementary Fig. S4E). Accordingly, DMF treatment triggered co-immunoprecipitation of caspase-8 with FADD and RIPK1 in CEM and SeAx cells (Fig. 3C, Supplementary Fig. S4F). Complex formation of caspase-8 and RIPK1 occurred 4–8 h after DMF exposure in SeAx cells and was most robust after 24 h in CEM cells (Fig. 3D; Supplementary Fig. S4G). To further establish that loss of NF $\kappa$ B activity triggered ripoptosome formation additional inhibitors of the NF $\kappa$ B signaling pathway (PMX464 and NBDII) were tested. Similar to DMF, PMX464 blocks NF $\kappa$ B activity by suppressing Trx1 (Supplementary Fig. S2A)<sup>28</sup>. NBDII (NEMO binding domain peptide) antagonizes the interaction of NEMO with the IKK complex and, therefore, suppresses NF $\kappa$ B activation. Administration of PMX464 and NBDII revealed that inhibition of the NF $\kappa$ B signaling pathway resulted in ripoptosome formation. Etoposide, which causes depletion of IAPs and subsequent ripoptosome-dependent cell death<sup>14</sup>, was used as positive control (Fig. 3C, Supplementary Fig. S4F).

Since DMF-mediated inhibition of NF $\kappa$ B resulted in decreased cIAP2 expression most efficiently, we tested whether knock-down of *Birc3* led to ripoptosome-dependent cell death. siRNA-mediated knock-down of about 60% resulted in moderate ripoptosome assembly and subsequent PCD (Fig. 3E). Thus, our data indicate that antagonizing NF $\kappa$ B activity induces ripoptosome formation, which is mediated by cIAP2 downregulation.

**Activation of the mitochondrial pathway is required for ripoptosome assembly and ripoptosome-dependent cell death.** IAPs are negative regulators of ripoptosome formation. cIAP2 was downregulated in response to DMF-dependent NF $\kappa$ B suppression, which resulted in ripoptosome assembly. To evaluate whether additional IAPs were involved in DMF-mediated assembly of the ripoptosome, we tested the role of cIAP1 and XIAP. cIAP1 and XIAP mRNA expression was not altered upon DMF administration (Supplementary Fig. S5A). However, protein expression was impaired in response to DMF after 4–8 h suggesting an additional mechanism that led to decreased protein levels of cIAP1 and XIAP (Supplementary Fig. S5B).

Caspase-8 can activate downstream effector caspases such as caspase-3 directly. Simultaneously, caspase-8 can induce Bid cleavage. Bid cleavage was observed 4–8 h after DMF administration (Supplementary Fig. S5C). Cleaved Bid results in MOMP and subsequent release of pro-apoptotic molecules such as cytochrome c and Smac<sup>31</sup>. Since Smac has been reported to promote degradation of IAPs, we tested whether Smac was released by mitochondria in response to NF $\kappa$ B inhibition. Indeed, DMF-mediated Smac release occurred most robustly after 4–8 h, which coincided with a decrease in cIAP1 and XIAP protein levels (Fig. 4A,B and Supplementary Fig. S5B). Release of Smac was caspase-dependent since inhibition of caspase-8 resulted in decreased Smac translocation from mitochondria (Fig. 4C). Moreover, inhibition of caspase-8 led to recovery of decreased protein expression levels of cIAP1 and XIAP but not cIAP2 (Fig. 4D). This is consistent with previous results showing that cIAP2 expression was regulated by NF $\kappa$ B activity (compare Fig. 2). Thus, downregulation of cIAP2 in response to DMF results in Smac release from the mitochondria and in degradation of XIAP and cIAP1.

Next, we evaluated whether Smac release and subsequent degradation of IAPs was necessary for ripoptosome-dependent cell death. Therefore, we used Bcl<sub>XL</sub> overexpressing cells (CEM<sup>Bcl<sub>XL</sub></sup>) and compared them with control CEM cells (CEM<sup>Neo</sup>). Bcl<sub>XL</sub> inhibits MOMP-dependent release of mitochondrial contents such as Smac. In CEM<sup>Neo</sup> cells DMF diminished mitochondrial membrane potential. In contrast, overexpression of Bcl<sub>XL</sub> abolished MOMP (Fig. 5A). Interestingly, Bcl<sub>XL</sub> overexpression diminished ripoptosome-dependent cell death suggesting that involvement of mitochondria is critical for DMF-mediated PCD (Fig. 5B). In concert, Bcl<sub>XL</sub> suppressed cleavage of caspase-9 and caspase-3 in response to DMF. Surprisingly, DMF administration resulted in reduced caspase-8 cleavage in CEM<sup>Bcl<sub>XL</sub></sup> cells. In addition, caspase-8-dependent RIPK1 cleavage was rescued by Bcl<sub>XL</sub> suggesting that mitochondria are critical for ripoptosome formation and subsequent cell death (Fig. 5C). Indeed, Bcl<sub>XL</sub> diminished complex formation of RIPK1/FADD/caspase-8 in response to DMF indicating an essential mitochondrial amplification loop, which promotes ripoptosome assembly (Fig. 5D).

To further characterize PCD we compared the effect of DMF with PMX464, etoposide, and LCL161. LCL161 is a Smac mimetic, which induces assembly of the ripoptosome by depleting IAPs<sup>32</sup>. Similar to DMF treatment, induction of MOMP in response to PMX464, etoposide, or LCL161 was diminished by Bcl<sub>XL</sub> (Fig. 5A). PCD was rescued by Bcl<sub>XL</sub> upon PMX464 or etoposide administration. However, LCL161 treated CEM<sup>Bcl<sub>XL</sub></sup> cells revealed moderate inhibition of PCD (Fig. 5B). This is in line with caspase cleavage and complex formation. Assembly of the ripoptosome and caspase cleavage upon LCL161 administration was only moderately inhibited suggesting that the Smac mimetic is less dependent on MOMP-mediated Smac release (Fig. 5C,D). In contrast, Bcl<sub>XL</sub> diminished complex formation and caspase cleavage in response to etoposide (Fig. 5C,D) indicating that both, DMF and etoposide require mitochondria for ripoptosome-dependent cell death. Thus, overexpression of Bcl<sub>XL</sub> inhibits mitochondrial Smac release and subsequent degradation of IAPs (e.g. cIAP1 and XIAP) in response to DMF. Collectively, these data suggest that reduction of cIAP2 in response to DMF-induced NF $\kappa$ B inhibition results in moderate ripoptosome formation. However, to enhance cell death, sufficient assembly and activation of the ripoptosome requires a caspase-8-dependent mitochondrial amplification loop characterized by MOMP and Smac-induced degradation of cIAP1 and XIAP.

**Ripoptosome-dependent cell death in human malignant T-cells occurs in an apoptotic and necroptotic manner.** CTCL, including its leukemic variant Sézary syndrome, is characterized by a CD4<sup>+</sup>, CD45RO<sup>+</sup> and CD8<sup>-</sup> phenotype and an elevated expression of constitutively active NF $\kappa$ B accompanied by resistance to PCD<sup>2,20,33</sup>. DMF is a potent inhibitor of NF $\kappa$ B activity and was reported to induce apoptosis in stimulated human T-cells<sup>34</sup>.

CD4<sup>+</sup> T-cells were isolated from Sézary patients (Supplementary Table 1), which revealed elevated levels of phosphorylated NF $\kappa$ B, cIAP2 and cFLIP compared to healthy controls (Supplementary Fig. S6A). To evaluate the

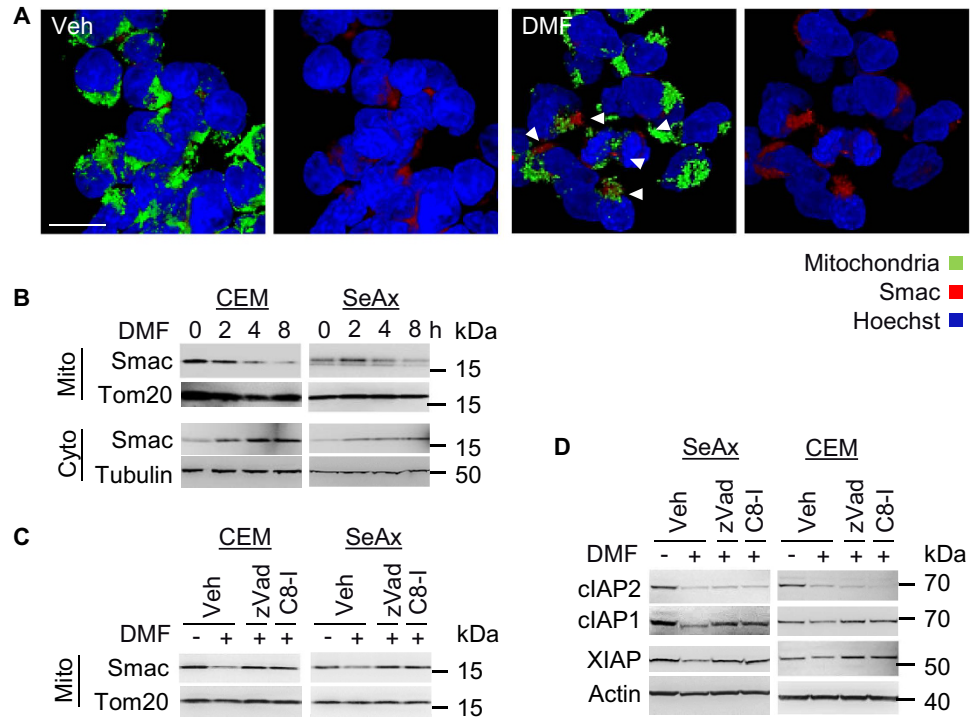


**Figure 4. DMF application induces Smac release.** (A) Shown are representative z-stacks of cells treated with DMSO (Veh) or DMF (50  $\mu$ M) for 8 h. Paraformaldehyde fixed cells were stained for Smac (red), mitochondria (green), Hoechst (blue), and analyzed by confocal microscopy; arrows indicate Smac release; scale bar, 10  $\mu$ m. (B) Mitochondria were isolated from DMF (50  $\mu$ M) treated cells as indicated. Cytoplasmic and mitochondrial fractions were analyzed by Western blot. (C) DMSO (Veh), zVad, and caspase-8 inhibitor (C8-I) incubated cells were left untreated or stimulated with DMF (50  $\mu$ M) for 8 h. Shown are Western blot analyses of isolated mitochondria (Mito). (D) Protein lysates of cells treated as described in (C) were analyzed for expression of cIAP2, cIAP1, XIAP and Actin.

impact of DMF treatment on malignant human T-cells, we first measured specific cell death of DMF-treated primary resting and malignant CD4<sup>+</sup> T-cells. NF $\kappa$ B inhibition by DMF led to increased PCD in T-cells isolated from Sézary patients (Fig. 6A). To determine the mode of cell death upon NF $\kappa$ B inhibition, apoptosis was distinguished from necroptosis by Annexin V-FITC/7AAD uptake (Fig. 6B,C). Interestingly, zVad protected resting CD4<sup>+</sup> cells from PCD but only marginally inhibited DMF-induced cell death in malignant T-cells. Here, zVad administration promoted necroptosis in almost all patient samples since zVad reduced the Annexin V-FITC positive population, but did not affect the appearance of double-positive cells. Only the combination of zVad with the RIPK1 inhibitor Necrostatin-1 (Nec-1) protected cells from DMF-induced PCD (Fig. 6B,C; Supplementary Fig. S6B). Similarly, inhibition of NF $\kappa$ B signaling by DMF, PMX464 or NBDII resulted in necroptotic cell death in CEM cells (Supplementary Fig. S6C,D). Thus, inhibitors of NF $\kappa$ B signaling can mediate necroptosis *via* the ripoptosome. LCL161<sup>35</sup>, which induces necroptosis in a variety of cell lines when treated together with zVad, was included as control (Supplementary Fig. S6C).

Consistent with the notion that malignant T-cells can die in an apoptotic or necroptotic manner, a similar mode of PCD was observed in stimulated T-cells (Supplementary Fig. S6E,F). PCD in response to DMF-dependent NF $\kappa$ B inhibition was elevated in stimulated T-cells (Supplementary Fig. S6E). In contrast to unstimulated T-cells, which exclusively die by apoptosis, PCD in stimulated T-cells was characterized by apoptosis and/or necroptosis upon caspase inhibition (Supplementary Fig. S6F), suggesting that stimulated as well as malignant T-cells share a similar phenotype revealing NF $\kappa$ B dependency. Furthermore, PCD was induced by ripoptosome formation because caspase-8 was complexed with RIPK1 upon DMF application in Sézary cells (Fig. 6D,E). Importantly, Sézary patients orally treated with DMF revealed substantial ripoptosome formation compared to untreated healthy donors (Fig. 6F). Moreover, caspase-3 cleavage was augmented in a majority of isolated CD4<sup>+</sup> cells from patient II indicating that DMF induces PCD in Sézary patients *via* the ripoptosome (Fig. 6G). Thus, application of DMF in Sézary patients may represent a promising approach for treatment of CTCL and other NF $\kappa$ B-dependent tumors.

## Discussion

NF $\kappa$ B is a promising target for treatment of lymphoproliferative diseases *e.g.* CTCL. So far a variety of NF $\kappa$ B Inhibitors have been tested such as Velcade<sup>®</sup>, curcumin and nonsteroidal anti-inflammatory therapeutics<sup>36–38</sup>. However, these drugs reveal limited therapeutic responses or are too toxic for clinical application. In contrast, DMF is a FDA approved drug used for treatment of psoriasis and multiple sclerosis displaying minor side effects.

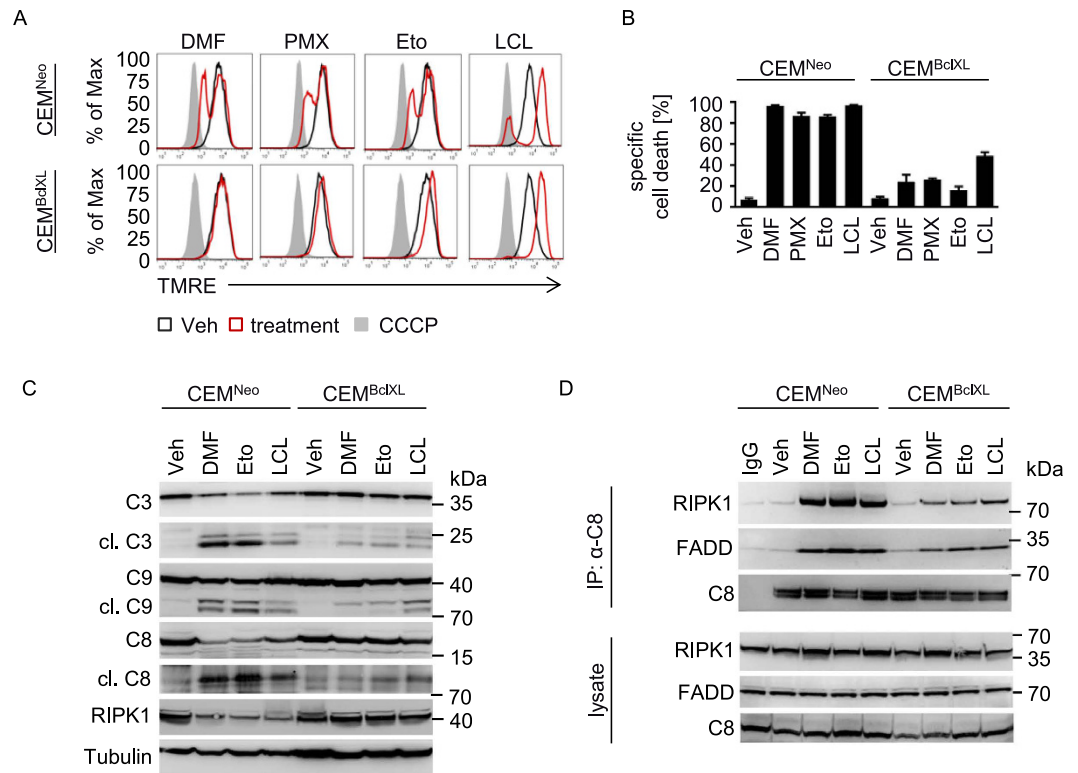


**Figure 5. A mitochondrial amplification loop promotes ripoptosome formation.** (A) CEM<sup>Neo</sup> or CEM<sup>BclXL</sup> cells were treated with DMF (50  $\mu$ M), PMX464 (PMX, 1  $\mu$ M), LCL161 (LCL, 20  $\mu$ M), or etoposide (Eto, 50  $\mu$ M) for 8 h (red). DMSO was used as vehicle control (black). CCCP was used as positive control (grey). MOMP was assessed by staining with TMRE. (B) Specific cell death was analyzed in cells stimulated with DMF (50  $\mu$ M), PMX464 (PMX, 1  $\mu$ M), LCL161 (LCL, 20  $\mu$ M), or etoposide (Eto, 50  $\mu$ M) for 18 h (n = 3). (C) CEM<sup>Neo</sup> or CEM<sup>BclXL</sup> cells were treated with DMSO (Veh), DMF (50  $\mu$ M), etoposide (Eto, 50  $\mu$ M), or LCL161 (LCL, 20  $\mu$ M) for 18 h. Lysates were subjected to Western blot and analyzed for caspase-3 (C3), -9 (C9), -8 (C8), RIPK1 and Tubulin. (D) Mitochondrial amplification loop promotes ripoptosome formation. Cells were pre-incubated with zVad and Nec-1, then stimulated as in (C) for 24 h. IP was performed with antibodies against caspase-8 ( $\alpha$ -C8). (B) Error bars represent standard deviation.

Previously, it has been shown that DMF application suppresses tumor growth and metastasis in a mouse CTCL xenograft model<sup>20</sup>. Therefore, it is of particular interest to investigate the inhibitory activity of DMF for the development of a novel class of improved NF $\kappa$ B inhibitors.

Here we show that therapeutic intervention targeting the NF $\kappa$ B signaling pathway in malignant T-cells results in cell death that is mediated by the ripoptosome. DMF has been reported to inhibit NF $\kappa$ B nuclear translocation, which leads to diminished production of pro-inflammatory cytokines and adhesion molecules<sup>39,40</sup>. Mechanistically, it was shown that DMF interferes with intracellular thiols<sup>40</sup>. Trx1 is a cellular redox scavenger, which is active when its reactive cysteine residues (C32, C35) are reduced<sup>41</sup>. Thioredoxin reductase 1 (TrxR1) can reduce oxidized C32 and C35 and, therefore, controls the activity of Trx1. The interaction of Trx1 and thioredoxin reductase is regulated by C73 another cysteine in vicinity to the postulated interaction side of both proteins<sup>24,26</sup>. Cancer cells often reveal elevated expression of active Trx1 and TrxR1, which maintains a reduced nuclear redox state providing an excellent environment for transcriptional activity<sup>42</sup>. We show that DMF modifies Trx1 at C73 leading to an inhibition of Trx1. NF $\kappa$ B is a redox-regulated transcription factor. Trx1 reduces NF $\kappa$ B in the nucleus and, thereby, enhances DNA-binding activity. Although it is possible that DMF influences other proteins apart from NF $\kappa$ B, depletion of IAPs coincided with the gene-induction profile upon NF $\kappa$ B inhibition. Loss of IAPs is associated with PCD triggered by DMF. Our experiments revealed that DMF-dependent induction of PCD was independent of death receptor engagement. Further, NF $\kappa$ B inhibition did not result in altered expression of death ligands such as TNF, CD95L and TRAIL in lymphoma cells. This indicates that the complex consisting of caspase-8, RIPK1 and FADD formed in response to NF $\kappa$ B inhibition is the intrinsic cell death platform called ripoptosome. In addition, our data indicate that a mitochondrial amplification loop improves ripoptosome formation in the T-ALL cell line CEM. This amplification loop is characterized by ripoptosome-dependent caspase-8 activity responsible for Smac-dependent degradation of IAPs and, thus, increased ripoptosome assembly (Supplementary Fig. S7). Therefore, it is likely that the extent of ripoptosome formation depends on induction of the mitochondrial amplification loop. In turn the amount of ripoptosome formation determines the extent of apoptotic and necroptotic cell death: Treatment with LCL161 (less dependent on the mitochondrial amplification loop) results in strong necroptotic cell death when caspase-8 is inhibited. In contrast, DMF or etoposide induce a weak ripoptosome initially. Caspase-8 activity is required to enhance assembly of the ripoptosome *via*

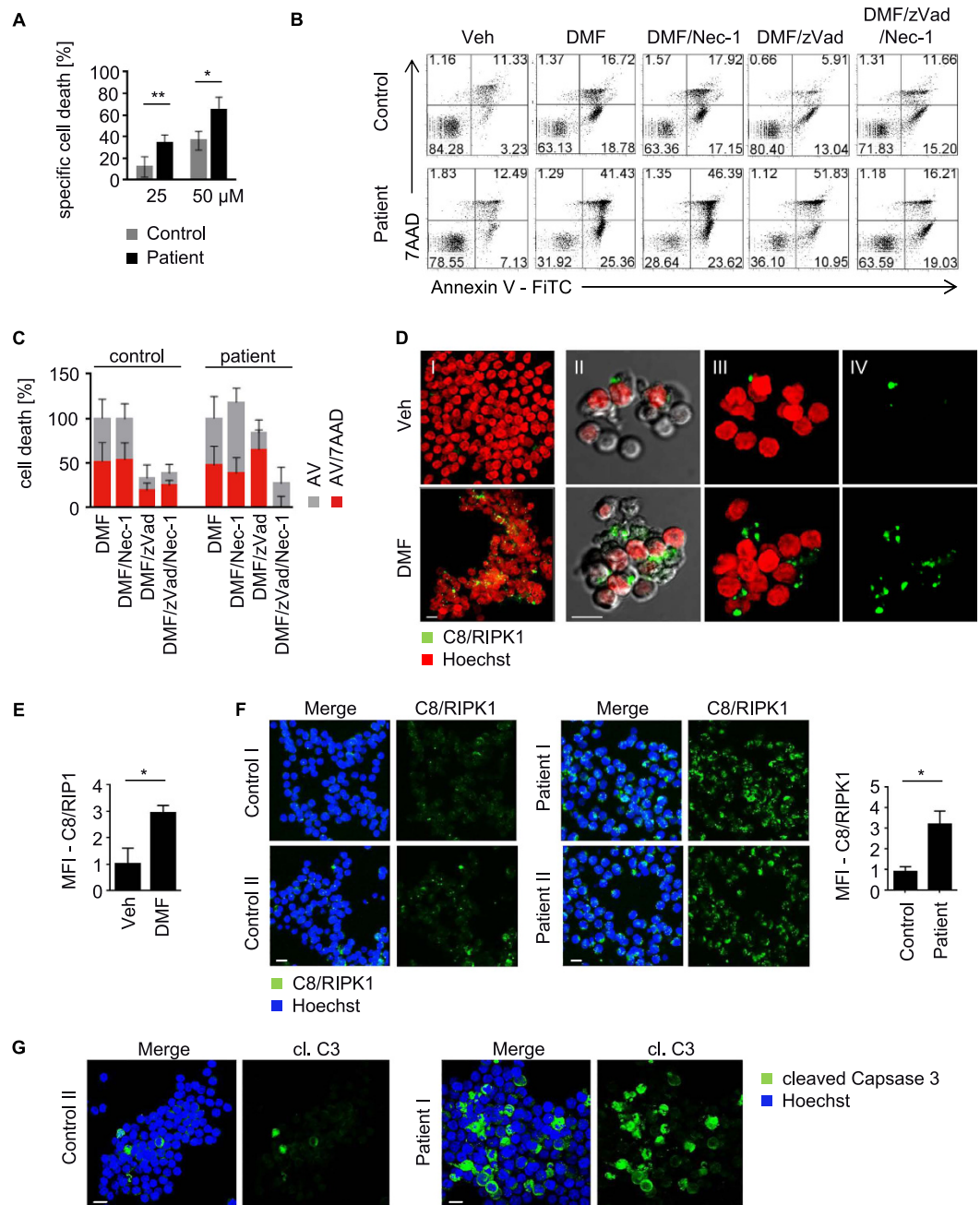


**Figure 6. DMF-dependent assembly of the ripoptosome augments cell death in human Sézary cells.** (A) Specific cell death of T-cells from healthy donors (control) and Sézary patients ( $n = 5$ ) treated with DMF ( $50 \mu\text{M}$ ) or vehicle control was assessed. (B) Isolated T-cells from CTCL-positive or -negative donors were stimulated as indicated, stained with AnnexinV-FITC and 7AAD, and analyzed by flow cytometry. (C) Quantification of AnnexinV-FITC (AV) and AnnexinV-FITC/7AAD (AV/7AAD) positive cells normalized to DMF treatment ( $n = 5$ ). (D) T-cells from Sézary patients ( $n = 2$ ) were stimulated with vehicle or DMF ( $50 \mu\text{M}$ ) for 24h. Complex formation of caspase-8 (C8) and RIPK1 (green) was determined by PLA, Hoechst (red); shown are representative immunofluorescences; scale bar:  $10 \mu\text{m}$  (I), z-stack, merge of C8/RIPK1 and Hoechst; (II) single plane image, merge of C8/RIPK1, Hoechst and Brightfield; (III) z-stack, merge of C8/RIPK1 and Hoechst; (IV) z-stack, C8/RIPK1. (E) Quantification of mean fluorescence intensities acquired from representative images as depicted in (D), ( $n = 3$ ). (F) Ripoptosome formation in DMF treated Sézary patients. Patient I and II were treated with  $480 \text{ mg/d}$  DMF for 26 and 10 weeks, respectively. Complex formation of RIPK1 and caspase-8 (C8) was determined by PLA in isolated  $\text{CD4}^+$  T-cells from DMF treated patients and healthy donors (Control I and II) and is depicted in green; nuclear staining with Hoechst is depicted in blue; shown are representative immunofluorescence analyses from z-stacks; scale bar,  $10 \mu\text{m}$ ; (left). Mean fluorescence intensities of PLA signals were quantified ( $n = 4$ ); (right). (G) Depicted are z-stacks from healthy donor (Control II) and DMF treated patient (patient I). Isolated  $\text{CD4}^+$  T-cells were stained for cleaved caspase-3 (cl. C3, green) and Hoechst (blue); scale bar,  $10 \mu\text{m}$ . (A,E,F) Error bars represent standard deviation. Statistics were calculated using Student's t-test (\* $p < 0.05$ ; \*\* $p < 0.005$ ; \*\*\* $p < 0.001$ ).

mitochondria. Accordingly, once caspase-8 activity is blocked by zVad, the mitochondrial amplification loop is lacking and ripoptosome formation is not augmented. Thus, induction of necroptosis upon zVad administration is less profound compared to LCL161 treated cells (Supplementary Fig. S8).

In summary, our observations show that inhibition of Trx1 results in diminished NF $\kappa$ B transcriptional engagement. DMF-dependent suppression of NF $\kappa$ B leads to downregulation of cIAP2 and cFLIP, which negatively regulate ripoptosome formation. Ripoptosome assembly is associated with caspase-8 activity, which promotes the mitochondrial amplification loop. This molecular mechanism provides important new information for prospective therapeutic interventions in cancer. Depending on the cellular context, elevated expression of anti-apoptotic Bcl-2 family members protecting mitochondria might dampen the ripoptosome-dependent response upon DMF administration. Thus, a combination of ripoptosome-inducing agents, such as Trx1 antagonists and inhibitors of Bcl-2 family members, might improve the anti-tumor responses.

Of note, non-stimulated T-cells exclusively die by apoptosis. In contrast, pre-activated as well as malignant CD4<sup>+</sup> T-cells, which share a similar phenotype, can die by necroptosis once caspase-8 activity is inhibited. This is in agreement with a report that necroptosis occurs as a result of antigen receptor-mediated activation in caspase-8 deficient T-cells<sup>13</sup>. The additional cell death pathway in form of necroptosis in pre-activated or malignant T-cells could point to an important checkpoint for T-cell homeostasis. Moreover, necroptosis has been implied to release massive amounts of damage-associated molecular patterns (DAMPs)<sup>43</sup>. Hence, necroptotic cell death of CTCL might trigger a strong inflammatory anti-tumor response.

Finally, our results demonstrate that inhibition of NF $\kappa$ B *via* Trx1 leads to ripoptosome formation and subsequent cell death in malignant T-cells. DMF exhibits only minor side effects compared to other anti-cancer drugs including Smac mimetics and therapeutic agents directly inhibiting NF $\kappa$ B. Therefore, targeting the Trx1 system including Trx1 and TrxR1 is a promising therapeutic approach. Accordingly, DMF represents a novel substance class of small-molecule inhibitors to treat lymphoproliferative diseases and other tumors with constitutive NF $\kappa$ B activation.

## Materials and Methods

**Chemicals.** Chemicals were obtained from Sigma unless otherwise indicated. Cells were treated with either zVad (25  $\mu$ M or 50  $\mu$ M, Bachem), Necrostatin-1 (Nec-1, 50  $\mu$ M), caspase-8 inhibitor (50  $\mu$ M, Merck), or respective combinations 30 min prior stimulation with either DMF, Etoposide (Biovision), LCL161 (Active Biochem), NBDII (Merck), PMX464 (Tocris) or TNF $\alpha$  (10 ng/ml) and Cycloheximide (Chx, 10  $\mu$ g/ml). Cells were incubated with 5  $\mu$ M carbonyl cyanide m-chlorophenyl hydrazone (CCCP) 10 min before measurement.

**Cells.** SeAx, HH and CEM cells were cultured in RPMI medium supplemented with 10% FCS and 0.1 mg/ml streptomycin or gentamycin. CEM<sup>Bcl<sub>XL</sub></sup> cells over-expressing Bcl<sub>XL</sub> and and CEM<sup>Neo</sup> control cells were selected with Neomycin<sup>44</sup>. The CTCL cell line HH and the ALL cell line CEM were originally from American Type Culture Collection (ATCC). SeAx cells were kindly provided by S. Eichmüller (German Cancer Research Center, Germany). Cells were tested by the cell contamination control unit of the DKFZ<sup>45</sup>.

**Antibodies.** Anti-caspase-8 monoclonal antibody C15 recognizes the p18 subunit of caspase-8. Anti-FLIP monoclonal antibody NF6 recognizes the N-terminal part of c-FLIP. Anti-FADD monoclonal antibody 1C4 recognizes the C-terminal part of FADD<sup>46</sup>. Antibodies against Caspase-3, caspase-9, p65, Phospho-NF $\kappa$ B p65 (Ser536), cIAP1, cIAP2, XIAP, Bcl<sub>XL</sub>, and Smac were obtained from Cell Signaling. Antibodies specific for Bcl-2 were purchased from Santa Cruz Biotechnology, RIPK1 from BD Bioscience, Trx and Tom20 from Abcam,  $\beta$ -Actin from Genetech and Tubulin from Sigma.

**Cell death assays and Luciferase activity assays.** Cell death was analyzed by FSC/SSC or Annexin V-FITC/7-Aminoactinomycin D (7AAD) staining using flow cytometry as described previously<sup>47</sup>. Specific cell death was calculated<sup>29</sup>. To determine mitochondrial membrane potential ( $\Delta\Psi_m$ ), cells were incubated with 50  $\mu$ M Tetramethylrhodamine ethyl ester (TMRE, Life Technologies) for 30 min. Caspase activity was measured using Caspase-Glo assay system (Promega) according to manufacturer's recommendations.

**Thioredoxin activity assay.** The Thioredoxin Activity Fluorescent Assay Kit (Cayman) uses fluorescence to measure active Trx in microtiter plates and was performed according to manufacturer's recommendations. The method is based on the reduction of insulin by reduced Trx.

**Immunoprecipitation and pull-down assays.** For co-immunoprecipitation of caspase-8 bound proteins, 1–2  $\times 10^7$  cells were pre-stimulated with zVad (25  $\mu$ M) 30 min prior to treatment with indicated substances. Caspase-8 was precipitated according to manufacturer's instructions (Promega). Equal amounts of eluates were analyzed by Western blot.

Two complementary biotinylated oligonucleotides containing NF $\kappa$ B binding sites were annealed and 1  $\mu$ g of double stranded oligonucleotides was incubated with 400  $\mu$ g of nuclear extracts in 500  $\mu$ l binding buffer (12% glycerol, 12 mM HEPES, pH 7.9, 4 mM Tris, pH 7.9, 150 mM KCl, 1 mM EDTA, 1 mM DTT, 0.1  $\mu$ g/ $\mu$ l poly (dI-dC) and 0.5  $\mu$ g/ $\mu$ l BSA). Protein complexes bound to each oligonucleotide were precipitated with preblocked streptavidin beads (Life Technologies), and analyzed by Western blot. For oligonucleotide sequences see Supplementary Information.

For pull-down of free thiols, cells were lysed with low pH buffer (50 mM 2-(N-morpholino) ethanesulfonic acid, pH 6.5), containing 1% Triton X-100 (v/v), 100 mM NaCl, and Complete-Mini protease inhibitor cocktail (Roche). Proteins containing free thiols incubated with biotinylated iodoacetamide (100  $\mu$ M, BIAM, Life technologies) were precipitated with 50  $\mu$ l Streptavidin beads pre-adsorbed with 1 mg/ml BSA. Proteins with accessible thiol groups were analyzed by Western blot.

**Immunofluorescence.** Immunofluorescent stainings and acquisition of mean fluorescence intensities (MFIs) were performed as described<sup>48</sup>. Primary antibodies (Smac, FADD (Abcam), caspase-8 (Santa Cruz), RIPK1 (BD Bioscience)), fluorophore-conjugated secondary antibodies and Hoechst33342 (Life Technologies) were diluted 1:50–1:100. For staining of mitochondria MitoTracker Deep Red (Life technologies) was added to secondary antibodies.

To visualize protein interactions a Proximity Ligation Assay (PLA) was performed according to manufacturer's recommendations (Sigma). Immunofluorescent stainings were analyzed by confocal microscopy (LSM710, Zeiss).

**Lymphocyte separation.** Human peripheral blood leukocytes were purified as described<sup>29</sup>. Then, T-cells were sorted with the CD4<sup>+</sup> T-Cell Isolation Kit II according to manufacturer's instruction (Miltenyi Biotec). The study was conducted according to ethical guidelines of the DKFZ and the Helsinki Declaration, and was approved by the ethics committee II of the Ruprecht-Karls-University of Heidelberg.

## References

- Kordes, U., Krappmann, D., Heissmeyer, V., Ludwig, W. D. & Scheidereit, C. Transcription factor NF-kappaB is constitutively activated in acute lymphoblastic leukemia cells. *Leukemia* **14**, 399–402 (2000).
- Sors, A. *et al.* Down-regulating constitutive activation of the NF-kappaB canonical pathway overcomes the resistance of cutaneous T-cell lymphoma to apoptosis. *Blood* **107**, 2354–2363, doi: 10.1182/blood-2005-06-2536 (2006).
- Vilimas, T. *et al.* Targeting the NF-kappaB signaling pathway in Notch1-induced T-cell leukemia. *Nature medicine* **13**, 70–77, doi: 10.1038/nm1524 (2007).
- Zhang, J., Chang, C. C., Lombardi, L. & Dalla-Favera, R. Rearranged NFKB2 gene in the HUT78 T-lymphoma cell line codes for a constitutively nuclear factor lacking transcriptional repressor functions. *Oncogene* **9**, 1931–1937 (1994).
- Karin, M., Cao, Y., Greten, F. R. & Li, Z. W. NF-kappaB in cancer: from innocent bystander to major culprit. *Nature reviews. Cancer* **2**, 301–310, doi: 10.1038/nrc780 (2002).
- Ghosh, S., May, M. J. & Kopp, E. B. NF-kappa B and Rel proteins: evolutionarily conserved mediators of immune responses. *Annu Rev Immunol* **16**, 225–260, doi: 10.1146/annurev.immunol.16.1.225 (1998).
- Kabe, Y., Ando, K., Hirao, S., Yoshida, M. & Handa, H. Redox regulation of NF-kappaB activation: distinct redox regulation between the cytoplasm and the nucleus. *Antioxid Redox Signal* **7**, 395–403, doi: 10.1089/ars.2005.7.395 (2005).
- Lillig, C. H. & Holmgren, A. Thioredoxin and related molecules--from biology to health and disease. *Antioxid Redox Signal* **9**, 25–47, doi: 10.1089/ars.2007.9.25 (2007).
- Micheau, O., Lens, S., Gaide, O., Alevizopoulos, K. & Tschopp, J. NF-kappaB signals induce the expression of c-FLIP. *Molecular and cellular biology* **21**, 5299–5305, doi: 10.1128/MCB.21.16.5299-5305.2001 (2001).
- Stehlik, C., de Martin, R., Binder, B. R. & Lipp, J. Cytokine induced expression of porcine inhibitor of apoptosis protein (iap) family member is regulated by NF-kappa B. *Biochemical and biophysical research communications* **243**, 827–832, doi: 10.1006/bbrc.1998.8185 (1998).
- Braun, T. *et al.* Targeting NF-kappaB in hematologic malignancies. *Cell death and differentiation* **13**, 748–758, doi: 10.1038/sj.cdd.4401874 (2006).
- Kaczmarek, A., Vandenabeele, P. & Krysko, D. V. Necroptosis: the release of damage-associated molecular patterns and its physiological relevance. *Immunity* **38**, 209–223, doi: 10.1016/j.immuni.2013.02.003 (2013).
- Chen, I. L., Tsau, J. S., Molkentin, J. D., Komatsu, M. & Hedrick, S. M. Mechanisms of necroptosis in T cells. *The Journal of experimental medicine* **208**, 633–641, doi: 10.1084/jem.20110251 (2011).
- Tenev, T. *et al.* The Ripoptosome, a signaling platform that assembles in response to genotoxic stress and loss of IAPs. *Molecular cell* **43**, 432–448, doi: 10.1016/j.molcel.2011.06.006 (2011).
- Feoktistova, M. *et al.* cIAPs block Ripoptosome formation, a RIP1/caspase-8 containing intracellular cell death complex differentially regulated by cFLIP isoforms. *Molecular cell* **43**, 449–463, doi: 10.1016/j.molcel.2011.06.011 (2011).
- Bertrand, M. J. & Vandenabeele, P. The Ripoptosome: death decision in the cytosol. *Molecular cell* **43**, 323–325, doi: 10.1016/j.molcel.2011.07.007 (2011).
- Vaux, D. L. & Silke, J. Mammalian mitochondrial IAP binding proteins. *Biochemical and biophysical research communications* **304**, 499–504 (2003).
- Vince, J. E. *et al.* IAP antagonists target cIAP1 to induce TNFalpha-dependent apoptosis. *Cell* **131**, 682–693, doi: 10.1016/j.cell.2007.10.037 (2007).
- Yang, Y., Fang, S., Jensen, J. P., Weissman, A. M. & Ashwell, J. D. Ubiquitin protein ligase activity of IAPs and their degradation in proteasomes in response to apoptotic stimuli. *Science* **288**, 874–877 (2000).
- Nicolay, J. P. *et al.* Dimethyl fumarate restores apoptosis sensitivity and inhibits tumor growth and metastasis in CTCL by targeting NFkappaB. *Blood*, doi: 10.1182/blood-2016-01-694117 (2016).
- Gerdes, S., Shakery, K. & Mrowietz, U. Dimethylfumarate inhibits nuclear binding of nuclear factor kappaB but not of nuclear factor of activated T cells and CCAAT/enhancer binding protein beta in activated human T cells. *Br J Dermatol* **156**, 838–842, doi: 10.1111/j.1365-2133.2007.07779.x (2007).
- Sullivan, L. B. *et al.* The proto-oncometabolite fumarate binds glutathione to amplify ROS-dependent signaling. *Molecular cell* **51**, 236–248, doi: 10.1016/j.molcel.2013.05.003 (2013).
- Gloire, G. & Piette, J. Redox regulation of nuclear post-translational modifications during NF-kappaB activation. *Antioxid Redox Signal* **11**, 2209–2222, doi: 10.1089/ARS.2009.2463 (2009).
- Haendeler, J. Thioredoxin-1 and posttranslational modifications. *Antioxidants & redox signaling* **8**, 1723–1728, doi: 10.1089/ars.2006.8.1723 (2006).
- Hashemy, S. I. & Holmgren, A. Regulation of the catalytic activity and structure of human thioredoxin 1 via oxidation and S-nitrosylation of cysteine residues. *The Journal of biological chemistry* **283**, 21890–21898, doi: 10.1074/jbc.M801047200 (2008).
- Gasdaska, J. R. *et al.* Oxidative inactivation of thioredoxin as a cellular growth factor and protection by a Cys73->Ser mutation. *Biochemical pharmacology* **52**, 1741–1747 (1996).
- Weichsel, A., Gasdaska, J. R., Powis, G. & Montfort, W. R. Crystal structures of reduced, oxidized, and mutated human thioredoxins: evidence for a regulatory homodimer. *Structure* **4**, 735–751 (1996).
- Callister, M. E. *et al.* PMX464, a thiol-reactive quinol and putative thioredoxin inhibitor, inhibits NF-kappaB-dependent proinflammatory activation of alveolar epithelial cells. *Br J Pharmacol* **155**, 661–672, doi: 10.1038/bjp.2008.258 (2008).
- Kiessling, M. K. *et al.* Inhibition of constitutively activated nuclear factor-kappaB induces reactive oxygen species- and iron-dependent cell death in cutaneous T-cell lymphoma. *Cancer research* **69**, 2365–2374, doi: 10.1158/0008-5472.CAN-08-3221 (2009).
- Ofengeim, D. & Yuan, J. Regulation of RIP1 kinase signalling at the crossroads of inflammation and cell death. *Nat Rev Mol Cell Biol* **14**, 727–736, doi: 10.1038/nrm3683 (2013).
- Kroemer, G., Galluzzi, L. & Brenner, C. Mitochondrial membrane permeabilization in cell death. *Physiol Rev* **87**, 99–163, doi: 10.1152/physrev.00013.2006 (2007).

32. Fulda, S. & Vucic, D. Targeting IAP proteins for therapeutic intervention in cancer. *Nat Rev Drug Discov* **11**, 109–124, doi: 10.1038/nrd3627 (2012).
33. Pichardo, D. A., Querfeld, C., Guitart, J., Kuzel, T. M. & Rosen, S. T. Cutaneous T-cell lymphoma: a paradigm for biological therapies. *Leuk Lymphoma* **45**, 1755–1765, doi: 10.1080/10428190410001693560 (2004).
34. Treumer, F., Zhu, K., Glaser, R. & Mrowietz, U. Dimethylfumarate is a potent inducer of apoptosis in human T cells. *The Journal of investigative dermatology* **121**, 1383–1388, doi: 10.1111/j.1523-1747.2003.12605.x (2003).
35. Rodriguez, D. A. *et al.* Characterization of RIPK3-mediated phosphorylation of the activation loop of MLKL during necroptosis. *Cell death and differentiation* **23**, 76–88, doi: 10.1038/cdd.2015.70 (2016).
36. Zhang, C. *et al.* Curcumin selectively induces apoptosis in cutaneous T-cell lymphoma cell lines and patients' PBMCs: potential role for STAT-3 and NF-kappaB signaling. *The Journal of investigative dermatology* **130**, 2110–2119, doi: 10.1038/jid.2010.86 (2010).
37. Zinzani, P. L. *et al.* Phase II trial of proteasome inhibitor bortezomib in patients with relapsed or refractory cutaneous T-cell lymphoma. *J Clin Oncol* **25**, 4293–4297, doi: 10.1200/JCO.2007.11.4207 (2007).
38. Braun, F. K. *et al.* Nonsteroidal anti-inflammatory drugs induce apoptosis in cutaneous T-cell lymphoma cells and enhance their sensitivity for TNF-related apoptosis-inducing ligand. *The Journal of investigative dermatology* **132**, 429–439, doi: 10.1038/jid.2011.316 (2012).
39. Loewe, R. *et al.* Dimethylfumarate inhibits TNF-induced nuclear entry of NF-kappa B/p65 in human endothelial cells. *Journal of immunology* **168**, 4781–4787 (2002).
40. Mrowietz, U. & Asadullah, K. Dimethylfumarate for psoriasis: more than a dietary curiosity. *Trends Mol Med* **11**, 43–48, doi: 10.1016/j.molmed.2004.11.003 (2005).
41. Jones, D. P. Radical-free biology of oxidative stress. *Am J Physiol Cell Physiol* **295**, C849–868, doi: 10.1152/ajpcell.00283.2008 (2008).
42. Go, Y. M. & Jones, D. P. Thioredoxin redox western analysis. *Curr Protoc Toxicol* Chapter 17, Unit17 12, doi: 10.1002/0471140856.tx1712s41 (2009).
43. Pasparakis, M. & Vandenabeele, P. Necroptosis and its role in inflammation. *Nature* **517**, 311–320, doi: 10.1038/nature14191 (2015).
44. Scaffidi, C. *et al.* Two CD95 (APO-1/Fas) signaling pathways. *The EMBO journal* **17**, 1675–1687, doi: 10.1093/emboj/17.6.1675 (1998).
45. Schmitt, M. & Pawlita, M. High-throughput detection and multiplex identification of cell contaminations. *Nucleic acids research* **37**, e119, doi: 10.1093/nar/gkp581 (2009).
46. Schleich, K. *et al.* Stoichiometry of the CD95 death-inducing signaling complex: experimental and modeling evidence for a death effector domain chain model. *Molecular cell* **47**, 306–319, doi: 10.1016/j.molcel.2012.05.006 (2012).
47. Abeler-Dorner, L. *et al.* Interferon-alpha abrogates the suppressive effect of apoptotic cells on dendritic cells in an *in vitro* model of systemic lupus erythematosus pathogenesis. *The Journal of rheumatology* **40**, 1683–1696, doi: 10.3899/jrheum.121299 (2013).
48. Schroeder, A. *et al.* Loss of androgen receptor expression promotes a stem-like cell phenotype in prostate cancer through STAT3 signaling. *Cancer research* **74**, 1227–1237, doi: 10.1158/0008-5472.CAN-13-0594 (2014).
49. Andersen, J. F. *et al.* Human thioredoxin homodimers: regulation by pH, role of aspartate 60, and crystal structure of the aspartate 60-> asparagine mutant. *Biochemistry* **36**, 13979–13988, doi: 10.1021/bi971004s (1997).
50. O'Donoghue, S. I. *et al.* Aquaria: simplifying discovery and insight from protein structures. *Nat Methods* **12**, 98–99, doi: 10.1038/nmeth.3258 (2015).

## Acknowledgements

We thank S. Pfrang, U. Matiba, D. Süß and T. Schlör for technical assistance, A. Kuhn for helpful discussions and the Sézary patients for blood donations. We thank Apogenix (Heidelberg, Germany) for a gift of APG101 and financial support from the 'Wilhelm-Sander-Stiftung' (2012.077.1) and the Helmholtz Alliance for Immunotherapy (HA-202).

## Author Contributions

Conception and design - A.S., K.G.; Development of methodology - A.S., K.G.; Acquisition of data - A.S., U.W., D.R., K.D.K., F.B., D.V., A.B. T.O.; Analysis of data - A.S., U.W., D.R., K.D.K., M.S., P.H.K., K.G.; Writing and review of the manuscript - A.S., P.H.K., K.G.; Administrative and material support - J.P.N.

## Additional Information

**Supplementary information** accompanies this paper at <http://www.nature.com/srep>

**Competing financial interests:** J.P.N., K.G. and P.H.K. received a consulting fee from Biogen.

**How to cite this article:** Schroeder, A. *et al.* Targeting Thioredoxin-1 by dimethyl fumarate induces ripoptosome-mediated cell death. *Sci. Rep.* **7**, 43168; doi: 10.1038/srep43168 (2017).

**Publisher's note:** Springer Nature remains neutral with regard to jurisdictional claims in published maps and institutional affiliations.



This work is licensed under a Creative Commons Attribution 4.0 International License. The images or other third party material in this article are included in the article's Creative Commons license, unless indicated otherwise in the credit line; if the material is not included under the Creative Commons license, users will need to obtain permission from the license holder to reproduce the material. To view a copy of this license, visit <http://creativecommons.org/licenses/by/4.0/>

© The Author(s) 2017